



The Journal of Biomedical Research

GSDMD protects intestinal epithelial cells against bacterial infections through its N-terminal activity impacting intestinal immune homeostasis

Li Honghui, Pu Jie, Yang Dongxue, Liu Lu, Hu Yingchao, Yang Shuo, Wang Bingwei

Cite this article as:

Li Honghui, Pu Jie, Yang Dongxue, Liu Lu, Hu Yingchao, Yang Shuo, Wang Bingwei. GSDMD protects intestinal epithelial cells against bacterial infections through its N-terminal activity impacting intestinal immune homeostasis[J]. *Journal of Biomedical Research*, In press. doi: 10.7555/JBR.38.20240041

View online: <https://doi.org/10.7555/JBR.38.20240041>

Articles you may be interested in

[H₂S protects against diabetes-accelerated atherosclerosis by preventing the activation of NLRP3 inflammasome](#)

The Journal of Biomedical Research. 2020, 34(2): 94 <https://doi.org/10.7555/JBR.33.20190071>

[SARS-CoV-2 encoded microRNAs are involved in the process of virus infection and host immune response](#)

The Journal of Biomedical Research. 2021, 35(3): 216 <https://doi.org/10.7555/JBR.35.20200154>

[Pleiotropic effects of apolipoprotein A- II on high-density lipoprotein functionality, adipose tissue metabolic activity and plasma glucose homeostasis](#)

The Journal of Biomedical Research. 2020, 34(1): 14 <https://doi.org/10.7555/JBR.33.20190048>

[Immune checkpoint inhibitors in cancer therapy](#)

The Journal of Biomedical Research. 2018, 32(5): 317 <https://doi.org/10.7555/JBR.31.20160168>

[Identification of therapeutic drugs against COVID-19 through computational investigation on drug repurposing and structural modification](#)

The Journal of Biomedical Research. 2020, 34(6): 458 <https://doi.org/10.7555/JBR.34.20200044>

[Function of flavonoids on different types of programmed cell death and its mechanism: a review](#)

The Journal of Biomedical Research. 2019, 33(6): 363 <https://doi.org/10.7555/JBR.33.20180126>



GSDMD protects intestinal epithelial cells against bacterial infections through its N-terminal activity impacting intestinal immune homeostasis

Honghui Li^{1,Δ}, Jie Pu^{2,Δ}, Dongxue Yang^{1,Δ}, Lu Liu¹, Yingchao Hu¹, Shuo Yang^{1,✉}, Bingwei Wang^{2,✉}

¹Department of Immunology, State Key Laboratory of Reproductive Medicine, Jiangsu Key Lab of Cancer Biomarkers, Prevention and Treatment, Collaborative Innovation Center for Personalized Cancer Medicine, Gusu School, the Affiliated Wuxi People's Hospital of Nanjing Medical University, Wuxi People's Hospital, Wuxi Medical Center, Nanjing Medical University, Nanjing, Jiangsu 211166, China;

²Department of Pharmacology, Nanjing University of Chinese Medicine, 138 Xianlin Avenue, Nanjing, Jiangsu 210023, China.

Abstract

The intestinal mucosal barrier serves as a vital guardian for gut health, maintaining a delicate equilibrium between gut microbiota and host immune homeostasis. Recent studies have found the intricate roles of Gasdermin D (GSDMD), a key executioner of pyroptosis downstream of the inflammasome, within the intestine, including controlling colitis in intestinal macrophage and the regulatory function in goblet cell mucus secretion. Thus, the exact role and nature of GSDMD's regulatory function in maintaining intestinal immune homeostasis and defending against pathogens remain elucidation. Here, we uncover that GSDMD plays a key role in defending against intestinal *Citrobacter rodentium* infection, with high expression in intestinal epithelial and lamina propria myeloid cells. Our results show that GSDMD specifically acts in intestinal epithelial cells to fight the infection, independently of its effects on antimicrobial peptides or mucin secretion. Instead, the resistance is mediated through GSDMD's N-terminal fragments, highlighting its importance in intestinal immunity. However, the specific underlying mechanism of GSDMD N-terminal activity in protection against intestinal bacterial infections still needs further study to clarify in the future.

Introduction

The intestinal mucosal barrier, consisting of biological, chemical, mechanical, and immune barriers, functions to defend against the invasion of external pathogens and ensure the stability of the intestinal microenvironment^[1]. The intestinal mucosal immune barrier acts as a critical line of defense

protecting the body from invading pathogens and is essential for maintaining the balance of gut microbiota and mucosal immune homeostasis^[2]. During intestinal bacterial infection, pattern-recognition receptors (PRRs) on intestinal epithelial cells (IECs) recognize pathogen-associated molecular patterns (PAMPs) and become activated, leading to the production of inflammatory factors and other immune defense

^ΔThese authors contributed equally to this work.

[✉]Corresponding authors: Shuo Yang, Department of Immunology, State Key Laboratory of Reproductive Medicine, Jiangsu Key Lab of Cancer Biomarkers, Prevention and Treatment, Collaborative Innovation Center for Personalized Cancer Medicine, Gusu School, the Affiliated Wuxi People's Hospital of Nanjing Medical University, Wuxi People's Hospital, Wuxi Medical Center, Nanjing Medical University, Nanjing, 101 Longmian Avenue, Jiangsu 211166, China. E-mail: shuoyang@njmu.edu.cn; Bingwei Wang, Department of Pharmacology, Nanjing University of Chinese Medicine, 138 Xianlin Avenue, Nanjing, Jiangsu 210023, China.

E-mail: bingweiwang@njucm.edu.cn.

Received: 18 February 2024; Revised: 29 March 2024; Accepted: 30 April 2024;

CLC number: R392.1, Document code: A

The authors reported no conflict of interests.

This is an open access article under the Creative Commons Attribution (CC BY 4.0) license, which permits others to distribute, remix, adapt and build upon this work, for commercial use, provided the original work is properly cited.

molecules, thereby promoting mucosal immune response^[3].

Inflammasomes are key inflammatory protein machines of the innate immune system, with core components such as NOD-like receptors that can sense various infections and endogenous danger signals, leading to the activation of inflammatory responses^[4]. The Inflammasome participates in host defense responses against pathogens, and play a crucial role in maintaining intestinal immune homeostasis^[5-6].

Gasdermin D (GSDMD) is a key executioner of pyroptosis downstream of the inflammasome^[7-9]. Upon activation by PAMPs signals through canonical or non-canonical pyroptosis pathways, the activated N-terminal fragment of GSDMD targets the cell membrane and oligomerizes to form pores, thereby exerting biological functions through pyroptosis or non-pyroptosis pathways^[7,10-12]. GSDMD plays a critical role in numerous immunoinflammatory diseases such as sepsis, neurodegenerative diseases, inflammatory bowel disease, atherosclerosis, and cancer^[13-23].

Recently, Zhang et al. reported the role of GSDMD in the intestinal epithelium, where it regulates goblet cell mucus secretion to maintain the intestinal mucosal barrier^[24]. Our previous research revealed that GSDMD in intestinal macrophages controls colitis by regulating cGAS-mediated inflammatory responses^[25]. These findings underscore the complex and multifaceted nature of GSDMD's regulatory functions in maintaining intestinal immune homeostasis and defending against pathogens. The exact role of GSDMD function in defending against pathogens remains elucidation.

In our current study, we have made a noteworthy discovery that GSDMD plays a unique protective role against intestinal bacterial infections exclusively within intestinal epithelial cells, rather than resident macrophages, and remarkably, this safeguarding function of GSDMD operates independently of its impact on the expression of antimicrobial peptides or the secretion of mucus proteins but depends on its N-terminal active fragment.

Materials and methods

Mice

Male mice with the C57BL/6 background were used in this study. The *Gsdmd*^{-/-} mice were kindly provided by F. Shao (National Institute of Biological Sciences, China). The *Villin*-CreERT mice were kindly provided by Dr. Yeguang Chen (Tsinghua University, China). The *Asc*^{-/-} mice were a gift from

V. Dixit (Genentech). The *Gsdmd*^{fl/fl} and the *Gsdmd*-NT^{F/+} mice were generated using conditional gene targeting methods by Cyagen Biosciences Inc. (Guangzhou, China) as described previously^[12,21]. For the *Gsdmd*-NT^{F/+} mice, the donor DNA containing 3×Flag *Gsdmd*-N fragment with LoxP-flanked stop cassette, the gRNA to mouse ROSA26 gene and CAS9 mRNA were co-injected into the C57BL/6 zygotes to generate targeted knock-in offspring. *Gsdmd*-floxed mice were crossed with *lysozyme M*-Cre mice (*Lysm*-Cre; the Jackson laboratory) to generate myeloid cell-conditional *Gsdmd* knockout mice (*Gsdmd*^{fl/fl} *Lysm*-Cre) or with *Villin*-Cre mice (the Jackson laboratory) to produce IEC-conditional *Gsdmd* knockout mice (*Gsdmd*^{fl/fl} *Villin*-Cre). *Gsdmd*-NT^{F/+} mice were crossed with *Villin*-CreERT mice to produce IEC-conditional *Gsdmd* knockin mice (*Gsdmd*-NT^{F/+} *Villin*-CreERT). *Gsdmd*-NT^{F/+} *Villin*-CreERT mice were crossed with *Gsdmd*^{-/-} mice to produce IEC-conditional *Gsdmd* rescue mice. In order to induce the activity of Cre, male mice aged 8-10 weeks was injected intraperitoneally with 300 μl Tomoxifen (10 mg/mL) five days before the establishment of *C. rodentium* infection model. All mice were kept in a barrier facility, and all animal experiments were conducted in accordance with the procedure approved by the Ethical Review Committee for Laboratory Animal Welfare of the Nanjing Medical University and Nanjing University of Chinese Medicine.

Reagents and materials

C. rodentium (51 459, ICC80) was obtained from ATCC (Manassas, VA, USA). Potassium salt was purchased from Sciencelight (luc001, Shanghai, China). Tris, Igepal, glycerol, NaF, Na₃VO₄, dithiothreitol, NaCl, Anhydrous ethanol, xylene, neutral gum, hydrochloric acid, and paraformaldehyde were sourced from Sinopharm Chemical Reagent Co., Ltd (Shanghai, China). Agarose was supplied by Yeasen (10208ES60, Shanghai, China). Yeast extract (LP0021) and Tryptone (LP0042) were provided by OXOID (Waltham, MA, USA). Phenylmethylsulphonyl fluoride (52 332), Nalidixic acid (N8878), Hematoxylin (HHS32), Eosin (E4382), and protease inhibitor cocktail (P8340) were obtained from Sigma-Aldrich (City of Saint Louis, MO, USA). Streptomycin sulfate was sourced from Ameresco (S0382, Framingham, MA, USA). TRIzol reagent was purchased from Invitrogen (15596026, Carlsbad, CA, USA). AceQ qPCR SYBR Green Master Mix was purchased from Vazyme (Q131-02/03, Nanjing, China). Gentamycin was purchased from Sangon Biotech (B540724-0010, Shanghai, China).

Kanamycin sulfate was obtained from Biosharp (0408, Anhui, China). Anti-IL-6 (Dy406), anti-TNF- α (DY410), and anti-MCP-1 (DY479) ELISA kits were provided by R&D Systems (Minneapolis, MN, USA). PAS staining solution was sourced from Wuhan Guge Biological Technology Co., Ltd (Wuhan, China). Anti-EPCAM (567664, 1 : 200) and CX3CR1 (567805, 1 : 500) were purchased from BD Biosciences (Sussex, NJ, USA). Anti-CD45-AF700 (56-0451-82, 1 : 400) and anti-CD326-APC (17-5791-80, 1 : 400) were purchased from eBioscience (Santiago, CA, USA).

***C. rodentium* bacterial culture**

The *C. rodentium* strain was propagated overnight on agar plates, then a single clone of UPEC was isolated and inoculated in lysogeny broth (LB) agar medium (containing Kanamycin sulfate and nalidixic acid) until it grew to an exponential phase (OD₆₀₀=0.5–1.0). The cells were centrifuged at 4000 rpm for 10 minutes at 4 °C, and the pellets were washed once with pre-cooled phosphate-buffered saline (PBS) and then stored in PBS.

Optical imaging *in vivo*

8 to 10 weeks mice were deprived of food and water for 4 hours before gavaged with 25 mg Streptomycin sulfate. After 24 hours, the mice were deprived of food and water for another 4 hours before gavaged with bioluminescent *C.rodentium* (ICC180) (2x10⁹ CFU). Then, the mice give normal diet 4 hours later to establish enteritis model. On the 9th day post intragastric administration, the mice were subjected to optical imaging *in vivo*, and IVIS Spectrum instrument (Caliper, PerkinElmer) was used to collect images and livingImages4.3.1 software for data analysis.

Bacterial load test

On the 15th day after intragastric administration of *C. rodentium* (ICC180), the organs (mesenteric lymph nodes, spleen, liver) were collected, weighed, and then added with sterile PBS and ground with ceramic beads under sterile conditions. After grinding, the cells were centrifuge at 3500 rpm and start coating. After the coating is completed, invert the culture dish at 37 °C overnight to observe the bacterial growth and make statistics.

HE staining

Colon tissue was fixed in 4% paraformaldehyde solution for more than 24 hours. The tissue was dehydrated, transparent, and immersed in wax before

being embedded in paraffin and sectioned into paraffin tissue. After routine dewaxing and rehydration with xylene and gradient alcohol from high to low, rinse with tap water for 5 minutes; stain the sections with hematoxylin staining solution for 3 minutes, rinse with tap water for 5 minutes, differentiate with 1% hydrochloric acid alcohol for 3-5 seconds, rinse with running water for 5-10 minutes, turn blue with ammonia, rinse with tap water for 5 minutes; stain the tissue sections with eosin staining solution for 15 minutes, rinse with tap water for 2 minutes; then dehydrate through a low to high gradient of alcohol and xylene to make it transparent, and seal with neutral gum; take pictures with a microscope (Nikon50i) Collect images to analyze the degree of intestinal inflammatory cell infiltration and mucosal hyperplasia.

PAS staining

Colon tissue was fixed in 4% paraformaldehyde solution for more than 24 hours. The tissue was dehydrated, transparent, and immersed in wax before being embedded in paraffin and sectioned into paraffin tissue. Dip in Chevre staining solution in the dark for 45-60 minutes, rinse with tap water for 10 minutes; dip the sections in hematoxylin staining solution for 3 minutes, rinse with tap water for 5 minutes, differentiate with hydrochloric acid alcohol solution for 3-5 seconds, rinse with tap water for 5-10 minutes, and turn blue with ammonia. Rinse with tap water for 5 minutes; the stained tissue sections are dehydrated and made transparent by gradient alcohol and xylene from low to high, and sealed with neutral gum; images are collected and analyzed using a microscope (Nikon50i).

RT-qPCR

The colon tissue was collected and centrifuged. Total RNA was extracted by using TRIzol reagent (Invitrogen, USA) and subjected to cDNA synthesis. qRT-PCR was performed using AceQ qPCR SYBR Green Master Mix (Vazyme, China). The expression of a single gene was calculated by a standard curve method and standardized to the expression of Hprt.

ELISA

On the 15th day after intragastric administration of *C.rodentium* (ICC180), the colon tissue was weighed and homogenized. After grinding, the cells were centrifuged at 12,500 rpm at 4 °C. Conditional media were collected and measured by sandwich ELISA (R&D System, MN, USA), according to the manufacturer's instructions provided in the user manual.

Western blot

The colon tissue or BMDM cells were collected in lysis buffer (50 mM Tris-HCl, pH 7.4, containing 150 mM NaCl, 1% Igepal, 10% glycerol, 50 mM NaF, 1 mM Na_3VO_4 , 1 mM dithiothreitol, 1 mM phenylmethylsulphonyl fluoride, and complete protease inhibitor cocktail), followed by incubation for 40 min at 4 °C. Samples were quantified and resolved by SDS-PAGE, transferred to nitrocellulose membranes, and analyzed by immunoblot with the appropriate antibodies.

Isolation of colonic epithelial and immune cells and sorting

Colons were excised and washed thoroughly by flushing with PBS for several times. They were opened longitudinally and transferred into Gentle Cell Dissociation Reagent (STEMCELL, USA) and shaken for 20 minutes at 37 °C. The colons were then washed three times with PBS containing 2 mmol/L EDTA^[26]. All supernatants were collected and passed through a 100 mm cell strainer to get single-cell suspensions. The single-cell suspensions were collected and stained with anti-CD45 and anti-CD326. IECs ($\text{CD326}^+\text{CD45}^-$) were sorted on a BD FACSAria. The remaining colons were collected to digest for 45 minutes at 37 °C using Dulbecco's modified eagle medium (DMEM) containing 2% fetal bovine serum, collagenase IV (2.5 mg/mL; Sigma-Aldrich, SL, USA), and deoxyribonuclease I (10 U/mL; Roche, MA, USA). Single-cell suspensions were obtained by grinding through a 70 mm cell strainer. Subsequently, homogeneous cell suspensions were centrifuged over the Percoll density (GE Healthcare), and LP immune cells were separated by collecting the interface fractions between 40 and 80% percoll. After intensive washing, single-cell suspensions were stained with FVD eFlour 506, anti-CD45 and anti-CD326 for FACS sorting.

Statistical analysis

Data are presented as the mean \pm standard error of the mean (SEM). Samples were analyzed using unpaired t test or Mann Whitney test for two groups and ANOVA for multiple groups. In all cases, a P value of less than 0.05 was considered statistically significant.

Results

Protective role of GSDMD against colon *C. rodentium* infection

The *C. rodentium* infection model in mice is

commonly used to simulate human enteropathogenic *Escherichia coli* (EPEC) infection, which induces inflammatory and pathological responses similar to those caused by human enteropathogenic and enterohemorrhagic *Escherichia coli*. To investigate the role of GSDMD in host defense against intestinal bacterial infections, we used *C. rodentium* to infect *Gsdmd* knockout and WT mice, employing *Asc* (apoptosis-associated speck-like protein containing a CARD) knockout mice as a control. Previous study has demonstrated that *Asc* deletion aggravates *C. rodentium* infection in the colon of mice, promoting bacterial colonization^[27]. This phenotype makes *Asc*^{-/-} mice a valuable tool for comparing the effects of GSDMD deficiency on infection outcome. In our study, we used *C. rodentium* to infect both *Gsdmd* knockout and wild-type (WT) mice, with *Asc* knockout mice serving as a control. It was observed that, consistent with the phenotype of *Asc* knockout mice, *Gsdmd* knockout mice exhibited stronger and more widespread *C. rodentium* bioluminescent signals in the body at day 9 post-infection compared to WT mice (**Fig.1A**). On day 15 post-infection, *Gsdmd* knockout mice exhibited enhanced bacteria burden in colon, liver, mesenteric lymph nodes, and spleen (**Fig.1B**), as well as thickened colon mucosa, increased immune cell infiltration (**Fig.1C**), accompanied by elevated levels of the pro-inflammatory cytokines IL-6, MCP-1, and TNF- α (**Fig.1D**). These findings suggest that GSDMD plays a crucial role in resisting *C. rodentium* infections in the colon tract.

High expression of *Gsdmd* in colon epithelial and lamina propria myeloid cells

To investigate the protective role of GSDMD in the defense against *C. rodentium*, we used flow cytometry sorting to obtain colon epithelial cells ($\text{CD326}^+\text{CD45}^-$) and hematopoietic cells ($\text{CD45}^+\text{CD326}^-$) (**Fig.2A**). Subsequently, we verified the expression levels of *Villin*, representing epithelial cells, and CD45, representing myeloid cells, in these two cell populations using qPCR. The results confirmed the accuracy of our flow cytometry sorting (**Fig. 2B**). We also examined the expression and localization of GSDMD in the intestine and observed a notably high expression level of GSDMD in both colon epithelial cells and hematopoietic cells, which are critical components of intestinal mucosal immune system (**Fig.2B**). The results of Immunofluorescence, utilizing EPCAM and CX3CR1 as markers for staining epithelial cells and hematopoietic cells respectively, further demonstrated the distribution of GSDMD in both colon epithelial cells and lamina propria hematopoietic cells (**Fig.2C**).

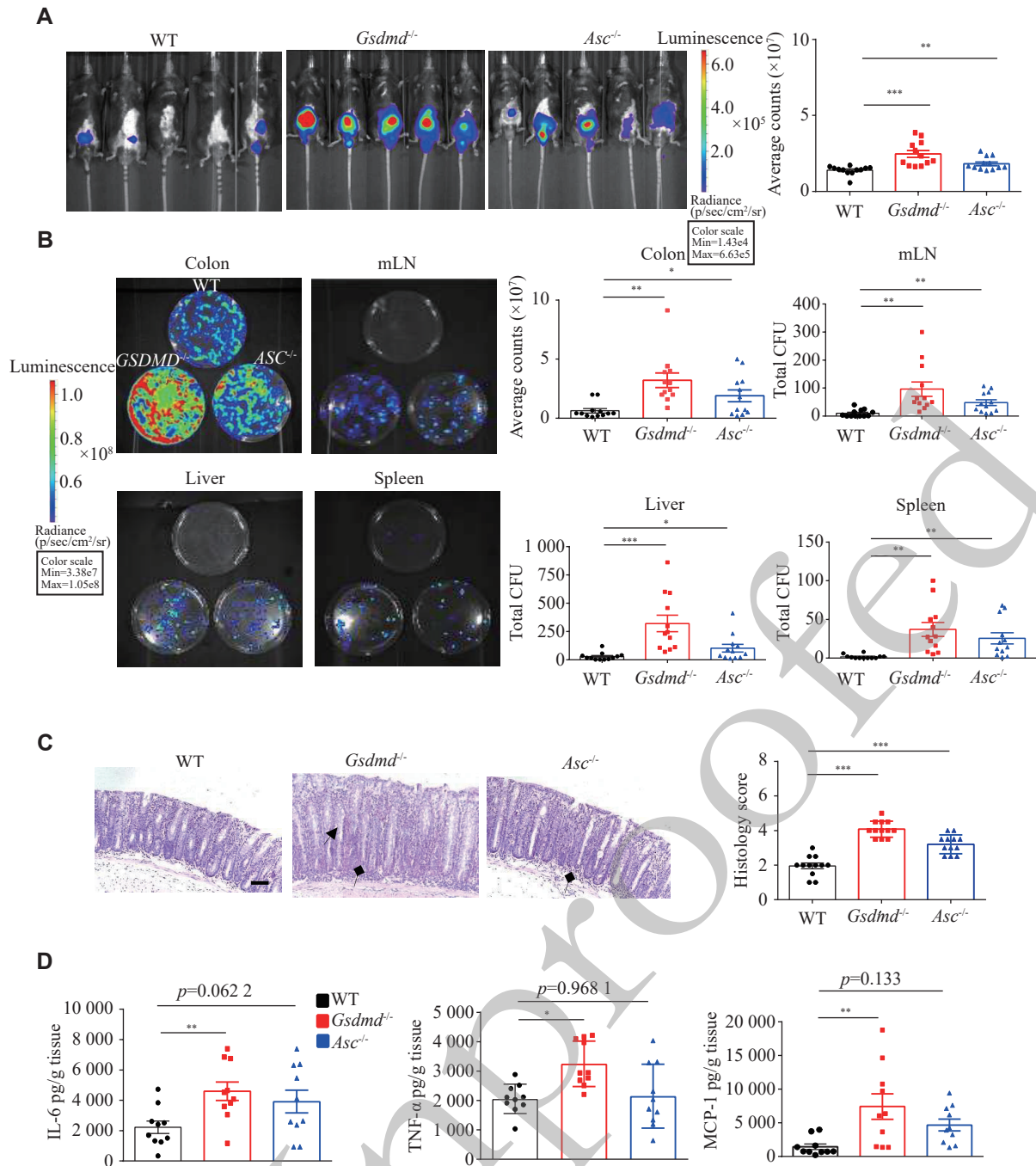


Fig. 1 GSDMD defends against *C. rodentium* Infection in the Intestine. A: Optical imaging in vivo analysis of the bacterial growth of WT, *Gsdmd*^{-/-} and *Asc*^{-/-} mice on the 9th day after intragastric administration of *C.rodentium*. Data are presented as a representative image (left) and quantified intensity (right) (n=12). B: Counts of bacterial colony in the colon, mesenteric lymph nodes, liver and spleen of WT, *Gsdmd*^{-/-} and *Asc*^{-/-} mice on the 15th day after intragastric administration of *C.rodentium* (n=12). C: Representative images and histological scores of H&E staining of colon pathological injury of WT, *Gsdmd*^{-/-} and *Asc*^{-/-} mice on the 15th day after intragastric administration of *C.rodentium*. Scale bars, 200 μ m (n=12). D: Elisa analysis of IL-6, TNF- α , MCP-1 in the colon supernatant of WT, *Gsdmd*^{-/-} and *Asc*^{-/-} mice on the 15th day after intragastric administration of *C.rodentium* (n=10). Data are pooled from three independent experiments (A-D). **p < 0.01, ***p < 0.001, ns, not significant. Unpaired t test for (A-D).

Functional defense of GSDMD against *C. rodentium* infection specifically in colon epithelial cells

GSDMD is primarily expressed in myeloid cells^[24]. Therefore, when GSDMD is knocked out in myeloid

cells using *Lysm*-Cre mice, there is essentially no GSDMD expression in the immune cells of these mice. To further elucidate the specific intestinal cells involved in GSDMD's defense against bacterial infection, we performed *C. rodentium* infection studies in conditional *Gsdmd* knockout mice in

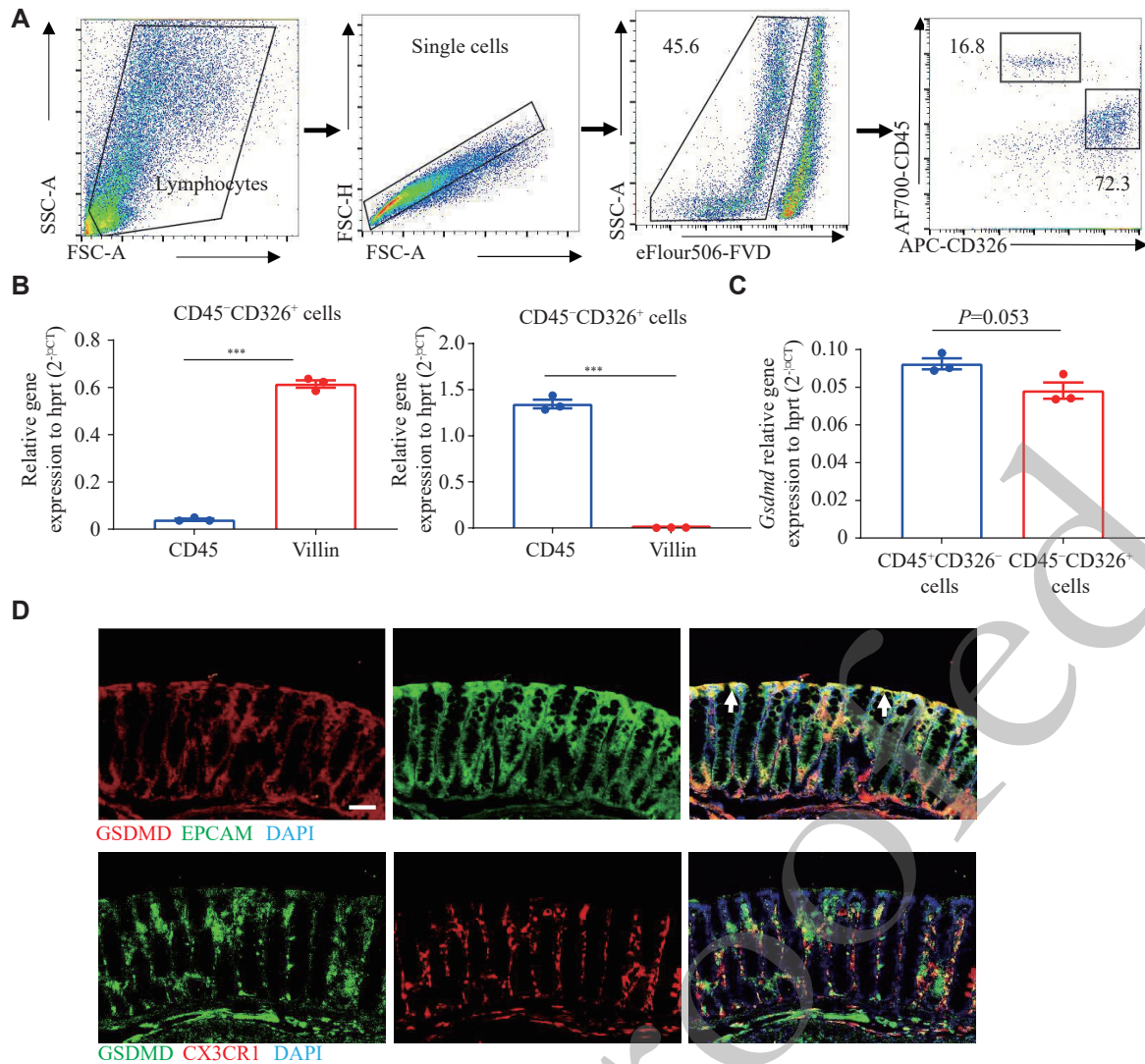


Fig. 2 GSDMD exhibits high expression in colon epithelial and lamina propria myeloid cells. A-C. QPCR analysis of the expression of *Gsdmd* in sorted intestinal epithelial cells and myeloid cells by flow cytometry (n=3). D. Immunofluorescence analysis of the distribution of GSDMD in colon epithelial cells and myeloid cells. Scale bars, 200 μ m. Data are pooled from three independent experiments (A-C) or are representative of three independent experiments (D). **p < 0.01, ***p < 0.001, ns, not significant. Unpaired t test for (B-C).

intestinal epithelial (*Villin-Cre*) and myeloid (*Lysm-Cre*) cells (Fig.3A). In vivo imaging results showed that, compared to the controls, *Gsdmd^{fl/fl}Villin-Cre* mice exhibited stronger and more widely distributed of *C. rodentium* bioluminescent signals on the 9th day post-infection (Fig.3B). On the 15th day post-infection, *Gsdmd^{fl/fl}Villin-Cre* mice demonstrated increased bacterial burden in the intestine, liver, mesenteric lymph nodes, and spleen (Fig.3C), along with thickened colon mucosa and enhanced immune cell infiltration (Fig.3D). In contrast, on the 9th day post-infection, *Gsdmd^{fl/fl}Lysm-Cre* mice showed no significant difference in *C. rodentium* bioluminescent signals compared to the controls (Fig.3E). And there was no significant difference between the colony burden of each tissue (Fig.3F) and the colonic pathological score in *Gsdmd^{fl/fl}Lysm-Cre* mice on day

15 post-infection (Fig.3G). Taken together, these findings indicate the critical protective role of GSDMD specifically within colon epithelial cells against intestinal bacterial infections.

Lack of effect of GSDMD on antimicrobial peptide and mucin secretion expression in colon epithelial cells

To gain insights into the underlying mechanisms by which GSDMD defends against bacterial infections, we first evaluated the expression of antimicrobial peptides and mucosal related proteins within the intestinal mucosa upon *C. rodentium* infection. Quantitative PCR (QPCR) analysis was conducted to assess the transcriptional expression of genes vital for colon epithelium function and immunity, namely *Reg3 beta*, *Reg3 gamma*, *Muc2*, *Dfn5*, *Lysozyme1*, and *Il22*.

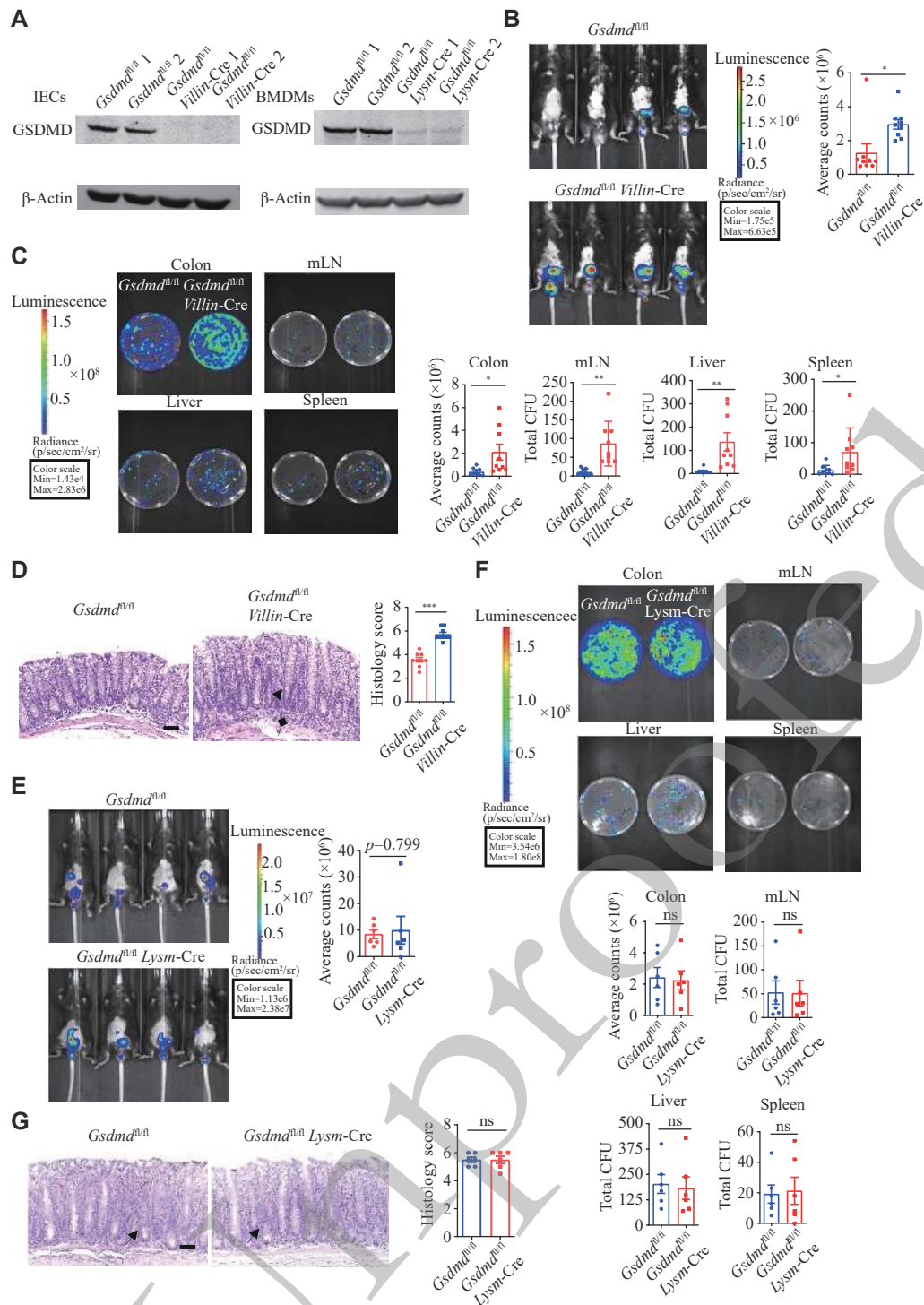


Fig. 3 GSDMD functions in defense against *C. rodentium* infection in colon epithelial cells. **A:** Immunoblot analysis of the knockout efficiency of GSDMD in colon epithelial cells and myeloid cells. **B:** Optical imaging in vivo analysis of the bacterial growth of *Gsdmd^{fl/fl}* and *Gsdmd^{fl/fl}Villin-Cre* mice on the 9th day after intragastric administration of *C.rodentium*. Data are presented as a representative image (left) and quantified intensity (right) (n=9). **C:** Counts of bacterial colony in the colon, mesenteric lymph nodes, liver and spleen of *Gsdmd^{fl/fl}* and *Gsdmd^{fl/fl}Villin-Cre* mice on the 15th day after intragastric administration of *C.rodentium* (n=9). **D:** Representative images and histological scores of H&E staining of colon pathological injury of *Gsdmd^{fl/fl}* and *Gsdmd^{fl/fl}Villin-Cre* mice on the 15th day after intragastric administration of *C.rodentium*. Scale bars, 200 μ m (n=12). **E:** Optical imaging in vivo analysis of the bacterial growth of *Gsdmd^{fl/fl}* and *Gsdmd^{fl/fl}Lysm-Cre* mice on the 9th day after intragastric administration of *C.rodentium*. Data are presented as a representative image (left) and quantified intensity (right) (n=6). **F:** Counts of bacterial colony in the colon, mesenteric lymph nodes, liver and spleen of *Gsdmd^{fl/fl}* and *Gsdmd^{fl/fl}Lysm-Cre* mice on the 15th day after intragastric administration of *C.rodentium* (n=6). **G:** Representative images and histological scores of H&E staining of colon pathological injury of *Gsdmd^{fl/fl}* and *Gsdmd^{fl/fl}Lysm-Cre* mice on the 15th day after intragastric administration of *C.rodentium*. Scale bars, 200 μ m (n=6). Data are representative of three independent experiments (A) or are pooled from three independent experiments (B-G). **p < 0.01, ***p < 0.001, ns, not significant. Unpaired t test for (B-G).

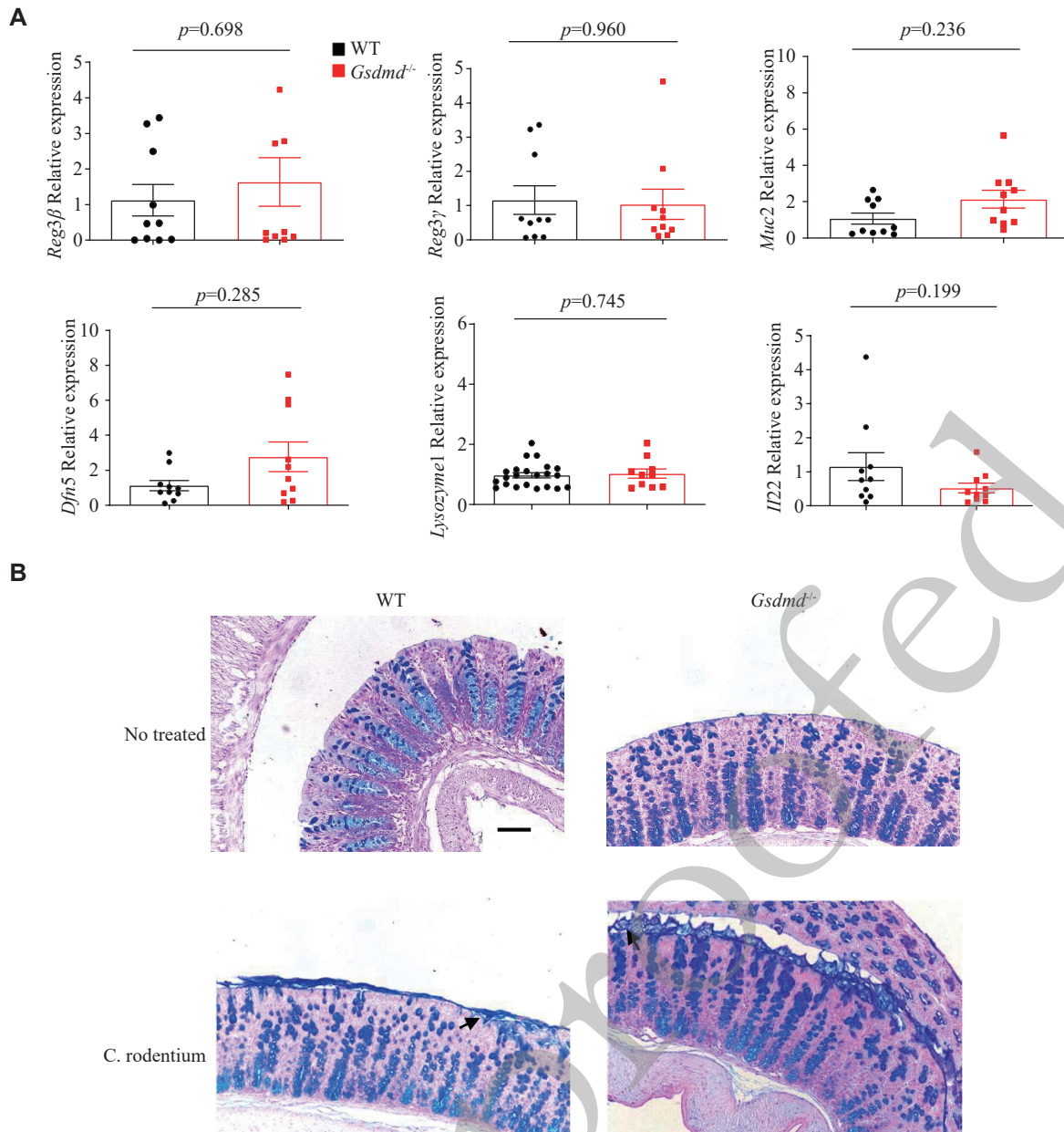


Fig. 4 GSDMD does not affect the expression of antimicrobial peptides and mucin secretion in colon epithelial cells. A. QPCR analysis of the expression of colon antimicrobial peptides of WT and *Gsdmd*^{-/-} mice (n=9). B. PAS staining analysis of the secretion of colon microbiota of WT and *Gsdmd*^{-/-} mice. Scale bars, 200 μ m. Data are pooled from three independent experiments (A) or are representative of three independent experiments (B). **p < 0.01, ***p < 0.001, ns, not significant. Unpaired t test for (A).

The results indicated that the deletion of GSDMD did not significantly impact the expression levels of these genes in the colon epithelium. (Fig.4A). This suggests that while GSDMD may play a role in intestinal immunity and epithelium function, its absence does not alter the baseline transcriptional expression of these critical genes.

Given the regulatory function of GSDMD in goblet cell mucin secretion^[24], and the crucial role of intestinal mucin in the formation of the intestinal epithelial barrier, which separates the epithelium from intestinal flora and wards off invading pathogens^[28], we next investigated the secretion of colon mucins in

response to *C. rodentium* infection. Surprisingly, Periodic Acid-Schiff (PAS) staining, a method used to detect mucin, demonstrated that the secretion of mucins by goblet cells remained unaffected by the absence of GSDMD (Fig.4B). These data indicate that GSDMD does not defend against bacterial infection by affecting the expression of antimicrobial peptides or secretion of mucus proteins.

GSDMD N-terminal fragments mediate resistance to *C. rodentium* infection in colon epithelial cells

Previous studies have reported that GSDMD

undergoes cleavage at Asp275 site to form a 22 kDa C-terminal fragment and a 31 kDa N-terminal fragment. The N-terminal fragment targets the plasma membrane and oligomerizes to form pores, thereby exerting its biological functions through pyroptosis or non-pyroptotic pathways^[24,29]. Next, we investigated the role of the GSDMD N-terminal fragment in colon epithelial cells in defense against pathogenic infections. We generated and employed mice with epithelial cell-specific knock-in expression of the GSDMD N-terminal fragment (*Gsdmd*-NT^{F/+}*Villin*-CreERT) and epithelial cell-specific rescue expression of the GSDMD N-terminal fragment in a *Gsdmd*-deficient background (*Gsdmd*^{-/-} + *Gsdmd*-NT^{F/+} *Villin*-CreERT). On the 9th day post-infection, compared to WT mice, *Gsdmd*-NT^{F/+}*Villin*-CreERT and *Gsdmd*^{-/-}+*Gsdmd*-NT^{F/+}*Villin*-CreERT mice exhibited weakened *C. rodentium* signals (**Fig.5A**). On the 15th day post-infection, these mice showed reduced bacterial burden in the colon and mesenteric lymph nodes (**Fig.5B**), lower colon tissue pathology scores (**Fig.5C**), and decreased bacterial colonization (**Fig.5D**). Collectively, these results suggest that the GSDMD in colon epithelial cells protects against intestinal *C. rodentium* infection through its N-terminal fragment.

Discussion

Growing evidence suggests that the inflammasome, an innate immune protein complex, is activated during intestinal pathogen infection and plays a critical role in the host's defense response and maintenance of intestinal immune homeostasis^[30]. GSDMD, a key mediator of pyroptosis downstream of the inflammasome, significantly impacts intestinal mucosal immunity and the onset of intestinal disease^[31]. Beyond its well-documented role in cell death, GSDMD has recently been implicated in processes that contribute to the integrity of the intestinal barrier. Zhang et al. discovered the involvement of GSDMD in cytoskeleton remodeling of goblet cells via actin regulation, which promotes mucous vesicle efflux under steady-state conditions^[24]. Our findings align with theirs in supporting the notion that Gasdermin protein does not impact the expression of intestinal mucosal proteins and is crucial for maintaining intestinal health. Recent research has revealed that *C. rodentium* can modulate host F-actin to establish a foundation, aiding its colonization and adhesion in the intestinal epithelium^[32]. It raises the possibility that during *C. rodentium* infection, GSDMD in intestinal epithelial cells might interfere with the formation of the host's actin base through its

N-terminal functional fragment, potentially influencing bacterial infection and colonization. However, further investigation is warranted to elucidate the precise mechanisms involved.

Besides, our previous study has added another layer of complexity to GSDMD's role in intestinal immunity. We found that GSDMD in intestinal macrophages regulates the onset of colitis and maintains intestinal immune homeostasis by modulating the cGAS-mediated inflammatory response^[25], suggesting the importance of GSDMD in fine-tuning the immune response in the intestine and preventing excessive inflammation.

Therefore, GSDMD has a complex regulatory role in maintaining the intestinal mucosal immune barrier against pathogen infection and preserving homeostasis. Further elucidation is required to determine the specific intestinal cell type through which GSDMD exerts its defensive function.

The present study further expands our understanding of GSDMD's role in intestinal immunity. It reveals that epithelial-specific GSDMD-deficient mice exhibit reduced defense against intestinal bacterial infection. Interestingly, this protective effect is mediated by GSDMD's N-terminal segment but is independent of its effect on antimicrobial peptide expression or mucin secretion. Thus, this suggests that GSDMD may have additional, hitherto unknown functions in non-immune cells that contribute to its protective effects against intestinal bacterial infection.

One potential mechanism by which GSDMD's N-terminal segment may exert its protective effect is through promoting the release of inflammatory mediators such as IL-1b and IL-18 by forming pyroptotic pores instead of cell death. These cytokines are known to play a crucial role in the host's defense against infection and could potentially be released through pores formed by GSDMD's N-terminal oligomerization. Miao et al. highlighted that this segment can also damage mitochondria, leading to the release of these cytokines, suggesting a role for mitochondrial dysfunction in GSDMD-mediated infection protection^[33]. Alternatively, GSDMD may regulate the expression or activity of other unknown antimicrobial molecules. Future studies are warranted to explore these possibilities and elucidate the precise molecular mechanism underlying GSDMD's protective effect.

In conclusion, our work has unveiled a new dimension to GSDMD's role in intestinal immunity. By protecting intestinal epithelial cells against bacterial infection through its N-terminal segment,

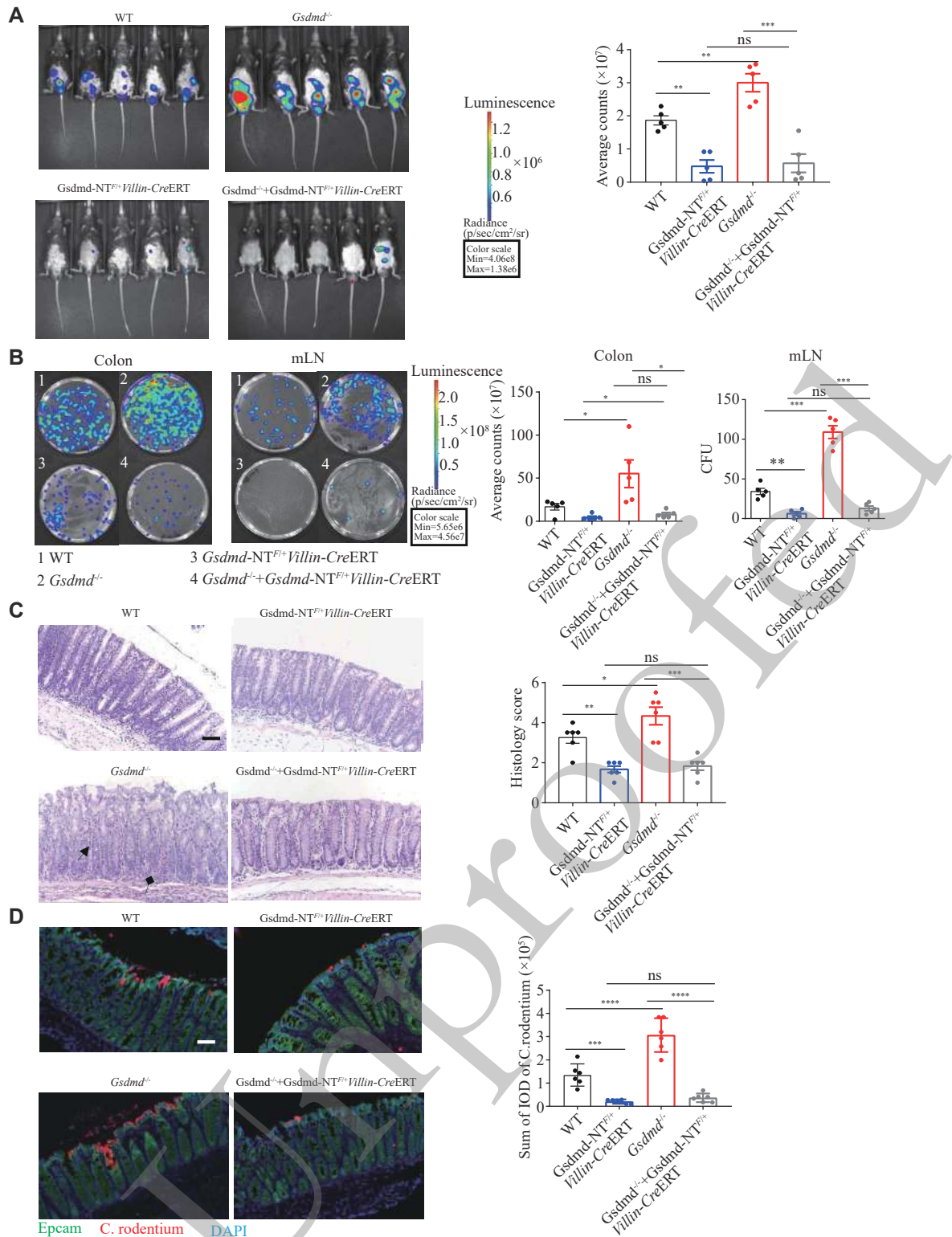


Fig. 5 GSDMD resists *C.rodentium* infection through N-terminal fragments in colon epithelial cells. A: Optical imaging in vivo analysis of the bacterial growth of WT, *Gsdmd*^{-/-}, *Gsdmd*-NT^{F/+}VillinCreERT and *Gsdmd*^{-/-}+*Gsdmd*-NT^{F/+}VillinCreERT mice on the 9th day after intragastric administration of *C.rodentium*. Data are presented as a representative image (left) and quantified intensity (right) (n=5). B: Counts of bacterial colony in the colon and mesenteric lymph nodes of WT, *Gsdmd*^{-/-}, *Gsdmd*-NT^{F/+}VillinCreERT and *Gsdmd*^{-/-}+*Gsdmd*-NT^{F/+}VillinCreERT mice on the 15th day after intragastric administration of *C.rodentium* (n=5). C: Representative images and histological scores of H&E staining of colon pathological injury of WT, *Gsdmd*^{-/-}, *Gsdmd*-NT^{F/+}VillinCreERT and *Gsdmd*^{-/-}+*Gsdmd*-NT^{F/+}VillinCreERT mice on the 15th day after intragastric administration of *C.rodentium*. Scale bars, 200 μ m (n=6). D: Immunofluorescence analysis of the colonic bacterial colonization of WT, *Gsdmd*^{-/-}, *Gsdmd*-NT^{F/+}VillinCreERT and *Gsdmd*^{-/-}+*Gsdmd*-NT^{F/+}VillinCreERT mice on the 15th day after intragastric administration of *C.rodentium*. Scale bars, 200 μ m (n=6). Data are pooled from three independent experiments (A-D). **p < 0.01, ***p < 0.001, ns, not significant. Unpaired t test for (A-D).

GSDMD emerges as a critical player in maintaining intestinal health and preventing intestinal bacterial infection. This study not only deepens our understanding of the formation and regulation of intestinal mucosal immunity but also may open up new avenues for the development of novel strategies to combat intestinal infections.

Fundings

This work was supported by the National Key Research and Development Program of China (2022YFA1303900 to S.Y.), National Natural Science Foundation of China (32 270 921 and 82 070 567 to S.Y. and 82 204 354 to Y.H.), the Open Project of State Key Laboratory of Reproductive Medicine of Nanjing Medical University (SKLRM-2021B3 to S.Y.), the talent cultivation project of "Organized scientific research" of Nanjing Medical University (NJMURC20220014 to S.Y.), the Natural Science Foundation of Jiangsu Province (BK20221352 to B.W.), the Jiangsu Provincial Outstanding Postdoctoral Program (2022ZB419 to Y.H.) and the Postdoctoral Research Funding Project of Gusu School (GSBSHKY202104 to Y.H.), the China Postdoctoral Science Foundation (2023T160329 to Y.H.)

Acknowledgments

None.

References

- [1] Camilleri M. Leaky gut: mechanisms, measurement and clinical implications in humans[J]. *Gut*, 2019, 68(8): 1516–1526.
- [2] Everard A, Belzer C, Geurts L, et al. Cross-talk between *Akkermansia muciniphila* and intestinal epithelium controls diet-induced obesity[J]. *Proc Natl Acad Sci USA*, 2013, 110(22): 9066–9071.
- [3] Brown EM, Sadarangani M, Finlay BB. The role of the immune system in governing host-microbe interactions in the intestine[J]. *Nat Immunol*, 2013, 14(7): 660–667.
- [4] Maslov LN, Naryzhnaya NV, Popov SV, et al. A historical literature review of coronary microvascular obstruction and intra-myocardial hemorrhage as functional/structural phenomena[J]. *J Biomed Res*, 2023, 37(4): 281–302.
- [5] Yao X, Zhang C, Xing Y, et al. Remodelling of the gut microbiota by hyperactive NLRP3 induces regulatory T cells to maintain homeostasis[J]. *Nat Commun*, 2017, 8(1): 1896.
- [6] Ahn H, Kwon HM, Lee E, et al. Role of inflammasome regulation on immune modulators[J]. *J Biomed Res*, 2018, 32(5): 401–410.
- [7] Shi J, Zhao Y, Wang K, et al. Cleavage of GSDMD by inflammatory caspases determines pyroptotic cell death[J]. *Nature*, 2015, 526(7575): 660–665.
- [8] Hu Y, Wang B, Li S, et al. Pyroptosis, and its role in central nervous system disease[J]. *J Mol Biol*, 2022, 434(4): 167379.
- [9] Naryzhnaya NV, Maslov LN, Popov SV, et al. Pyroptosis is a drug target for prevention of adverse cardiac remodeling: the crosstalk between pyroptosis, apoptosis, and autophagy[J]. *J Biomed Res*, 2022, 36(6): 375–389.
- [10] Kayagaki N, Stowe IB, Lee BL, et al. Caspase-11 cleaves gasdermin D for non-canonical inflammasome signalling[J]. *Nature*, 2015, 526(7575): 666–671.
- [11] He K, Wan T, Wang D, et al. Gasdermin D licenses MHCII induction to maintain food tolerance in small intestine[J]. *Cell*, 2023, 186(14): 3033–3048. e20.
- [12] Hu Y, Jiang Y, Li S, et al. The Gasdermin D N-terminal fragment acts as a negative feedback system to inhibit inflammasome-mediated activation of Caspase-1/11[J]. *Proc Natl Acad Sci USA*, 2022, 119(45): e2210809119.
- [13] Belkaid Y, Hand TW. Role of the microbiota in immunity and inflammation[J]. *Cell*, 2014, 157(1): 121–141.
- [14] Hotchkiss RS, Moldawer LL, Opal SM, et al. Sepsis and septic shock[J]. *Nat Rev Dis Primers*, 2016, 2: 16045.
- [15] Wellen KE, Hotamisligil GS. Inflammation, stress, and diabetes[J]. *J Clin Invest*, 2005, 115(5): 1111–1119.
- [16] Berg AH, Scherer PE. Adipose tissue, inflammation, and cardiovascular disease[J]. *Circ Res*, 2005, 96(9): 939–949.
- [17] Baumgart DC, Carding SR. Inflammatory bowel disease: cause and immunobiology[J]. *Lancet*, 2007, 369(9573): 1627–1640.
- [18] Glass CK, Saijo K, Winner B, et al. Mechanisms underlying inflammation in neurodegeneration[J]. *Cell*, 2010, 140(6): 918–934.
- [19] Greten FR, Grivnenkov SI. Inflammation and cancer: triggers, mechanisms, and consequences[J]. *Immunity*, 2019, 51(1): 27–41.
- [20] Wang B, Ma Y, Li S, et al. GSDMD in peripheral myeloid cells regulates microglial immune training and neuroinflammation in Parkinson's disease[J]. *Acta Pharm Sin B*, 2023, 13(6): 2663–2679.
- [21] Li S, Wu Y, Yang D, et al. Gasdermin D in peripheral myeloid cells drives neuroinflammation in experimental autoimmune encephalomyelitis[J]. *J Exp Med*, 2019, 216(11): 2562–2581.
- [22] Jiang Y, Yang Y, Hu Y, et al. Gasdermin D restricts anti-tumor immunity during PD-L1 checkpoint blockade[J]. *Cell Rep*, 2022, 41(4): 111553.
- [23] He W, Shi X, Dong Z. The roles of RACK1 in the pathogenesis of Alzheimer's disease[J]. *J Biomed Res*, 2024, 38(2): 137–148.
- [24] Zhang J, Yu Q, Jiang D, et al. Epithelial Gasdermin D shapes the host-microbial interface by driving mucus layer formation[J]. *Sci Immunol*, 2022, 7(68): eabk2092.

- [25] Ma C, Yang D, Wang B, et al. Gasdermin D in macrophages restrains colitis by controlling cGAS-mediated inflammation [J]. *Sci Adv*, 2020, 6(21): eaaz6717.
- [26] Jiang Y, Ma C, Hu Y, et al. ECSIT is a Critical factor for controlling intestinal homeostasis and tumorigenesis through regulating the translation of YAP protein[J]. *Adv Sci (Weinh)*, 2023, 10(25): 2205180.
- [27] Song-Zhao GX, Srinivasan N, Pott J, et al. Nlrp3 activation in the intestinal epithelium protects against a mucosal pathogen[J]. *Mucosal Immunol*, 2014, 7(4): 763–774.
- [28] Ashida H, Ogawa M, Kim M, et al. Bacteria and host interactions in the gut epithelial barrier[J]. *Nat Chem Biol*, 2012, 8(1): 36–45.
- [29] Sborgi L, Ruhl S, Mulvihill E, et al. GSDMD membrane pore formation constitutes the mechanism of pyroptotic cell death[J]. *EMBOJ*, 2016, 35(16): 1766–1778.
- [30] Zheng D, Liwinski T, Elinav E. Inflammasome activation and regulation: toward a better understanding of complex mechanisms[J]. *Cell Discov*, 2020, 6: 36.
- [31] Schwarzer R, Jiao H, Wachsmuth L, et al. FADD and caspase-8 regulate gut homeostasis and inflammation by controlling MLKL- and GSDMD-mediated death of intestinal epithelial cells[J]. *Immunity*, 2020, 52(6): 978–993. e6.
- [32] Scott SA, Fu J, Chang PV. Dopamine receptor D2 confers colonization resistance via microbial metabolites[J]. *Nature*, 2024, 628(8006): 180–185.
- [33] Miao R, Jiang C, Chang WY, et al. Gasdermin D permeabilization of mitochondrial inner and outer membranes accelerates and enhances pyroptosis[J]. *Immunity*, 2023, 56(11): 2523–2541. e8.

Unproofed